International Journal of Science and Research (IJSR)
ISSN (Online): 2319-7064
Index Copernicus Value (2013): 6.14 | Impact Factor (2014): 5.611

Effect on Properties of $ZnFe_2O_4$ Ferrites on Doping with Manganese Ions

Vikas J. Pissurlekar

Department of Chemistry, P.E.S.'s R.S.N College of Arts and Science, Ponda, Goa. - 403 401

Abstract: ***In the present study, a series of Zn ferrites doped with Mn having compositions of $Mn_x Zn_{(1-x)} Fe_2O_4$ (x=,0.4, 0.5, 0.6, 0.7 and 0.8) were synthesized from metal salts and succinate hydrazinate ligand precursors, by drying on a hot plate, which automatically got decomposed into the ferrite powders. The chemical interaction of ferrite powders was investigated by Fourier transform infra red spectroscopy (FTIR).The crystal structures and morphologies of these compounds were characterized by X-ray diffraction (XRD) and scanning electron microscopy (SEM), respectively. The single phase spinel cubic structure formation was confirmed by XRD and FTIR results. The magnetic properties of nanoparticles were measured at room temperature and indicate that the Mn content has a significant influence on the magnetic properties such as saturation magnetization and on Curie temperature.***

Keywords: Doped, ligand, precursors, nanoparticles, magnetic properties

1. Introduction

Ferrites are synthesized by many techniques such as ceramic, co-precipitation, hydrothermal, sol-gel, etc., also ball milling or mechanical alloying. However, most of these techniques have complicated synthesis steps, requires sophisticated instruments and take a long processing time [1]. Synthesis of ferrite using fuels such as urea, citric acid, glycine etc., in combustion method is well known [2, 3]. However, using a hydrazine based ligand to form a precursor with metal salts is tried in this synthesis. The technique involved is simple involving conventional heating using a hot plate and time required for synthesis is short and the product are obtained at a lower temperature. Among the spinel ferrites, zinc ferrite is being studied because of its unique properties such as chemical and thermal stability and the particle size dependence of magnetic properties [4]. Zinc ferrite in bulk state has a normal spinel structure with the Zn^{2+} ions without magnetic moment in the tetrahedral sites, and it behaves as antiferromagnetic. It is observed that method of preparation as well as crystallite size affects the magnetic properties of nanocrystalline zinc ferrite Nickel and manganese ferrites are kind of soft ferrimagnetic materials which have high saturation magnetization, high initial permeability, high resistivity, high dielectric constant and low power losses. As a result these materials have many applications such as electronic and computer devices, communication, space exploration and in the medical field [1,5]. Mn ions were doped in the zinc ferrite and the nanoparticles obtained were studied for their changes in structural, magnetic and electrical properties as mixed metal ferrites.

2. Experimental

Manganese Acetate, Zinc Nitrate, Ferric Nitrate chemicals of analytical grade were used in the synthesis. Manganese Acetate, Zinc Nitrate and Ferric Nitrate in stoichiometric amount were dissolved in minimum quantity of distilled water to obtain aqueous solution of metal ion. To this solution a calculated amount of Succinate hydrazinate ligand solution was added and it was thoroughly mixed to obtain a precursor. The mixture was then kept for drying on a hot plate. The solution dried to a solid mass, which automatically got decomposed into the powdered form and this powders were used for characterization and study of electrical and magnetic properties.

The phase formation of ferrite materials was investigated by X-ray diffraction (XRD). The chemical vibrational mode of ferrite samples was studied by Fourier transform infrared spectroscopy (FTIR). The morphology analysis of the samples was carried out by scanning electron microscopy (SEM). The saturation magnetization measurements of all the samples were carried out at room temperature using Pulse Field Magnetic Hysteresis Loop Tracer. Magnetization, coercivity and remanence magnetization were calculated from the hysteresis loops.

3. Results and Discussion

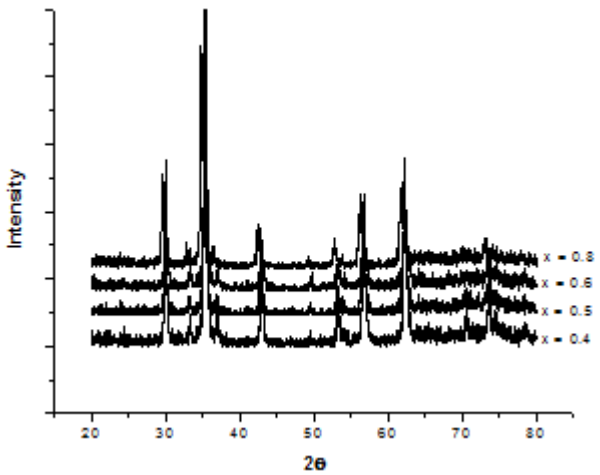

Figure 1: XRD pattern of $Mn_xZn_{(1-x)}Fe_2O_4$ samples

Figure 1 shows the X-ray diffraction patterns of samples $Mn_xZn_{(1-x)}$ Fe_2O_4, where x= 0.4, 0.5, 0.6, 0.7 and 0.8. All the peaks of all samples show the characteristic reflections of spinel cubic crystal structure of ferrite. The crystallite size (T), and lattice parameter (a) of all ferrite samples were calculated from the X-ray peak broadening of the characteristic (311) diffraction peak. Formation of single phase cubic spinel structure of $Mn_{(x)}Zn_{(1-x)}Fe_2O_4$ with x=

0.4/0.5/0.6/0.7/0.8 was confirmed with the help of XRD patterns obtained for all the samples. As shown in Table 1. The values of lattice constants ‚a" calculated from these were found to increase with increasing Mn concentration [6] and are in excellent agreement with reported values.

Table 1: Variation of lattice constant

Composition	a in A^0
$Mn_{0.4}Zn_{0.6}Fe_2O_4$	8.4219
$Mn_{0.5}Zn_{0.5}Fe_2O_4$	8.4431
$Mn_{0.6}Zn_{0.4}Fe_2O_4$	8.4628
$Mn_{0.7}Zn_{0.3}Fe_2O_4$	8.4704
$Mn_{0.8}Zn_{0.2}Fe_2O_4$	8.4826

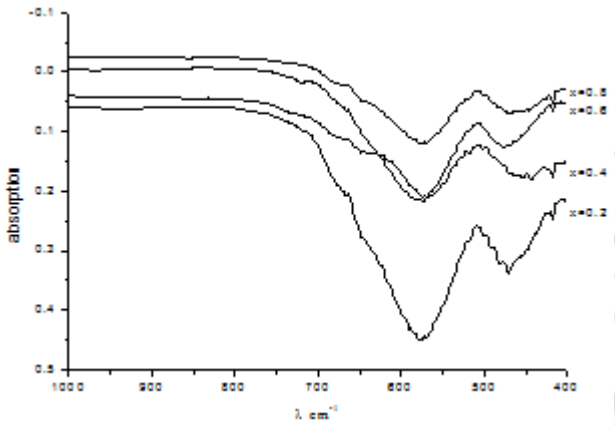

Figure 2: IR spectrum of $Mn_xZn_{(1-x)}Fe_2O_4$ samples

Infra red (IR) absorption spectroscopy helps to identify the spinel structure. The three typical vibrational bands associated with spinel structure [7] are at (1) 600-550cm^{-1} (2) 450-385 cm^{-1} (3) 350-330cm^{-1} for metal-oxygen band. Fourier transformed infra red (FTIR) spectroscopy studies of the nano particle ferrite samples were carried out between 1000 - 400 cm^{-1} as shown in figure 2. Out of the two bands the high frequency (υ_1) band is attributed to the tetrahedral metal-oxygen bond and second frequency (υ_2) band to the octahedral metal-oxygen bond corresponding to:
(1) $Me_T - O - Me_O$ stretching vibration 600-550 cm^{-1} (2) $Me_O \leftrightarrow O$ stretching vibration 450-385 cm^{-1} here O is oxygen, Me_O is metal in the octahedral site and Me_T in the tetrahedral site. The metal-oxygen absorption bands (1) and (2) are pronounced for all spinel structures and essentially for ferrites, which are also seen in these samples. IR spectral data of all the ferrite samples prepared by these methods are found to show two peaks in the range 578-564 cm^{-1} and 472-443 cm^{-1} which are in agreement with the reported value [8].

Average crystallite sizes were calculated by using XRD data by measuring the full-width at half maximum (FWHM) for most intense characteristic (311) peak for each sample with the help of the Scherer formula as given in equation 1, and are in the range 20.4-41.1 nm for different Mn concentrations.

$$T=0.9\,\lambda/Dp\cos\theta \qquad (1)$$

Where, T is the average crystallite size, λ is the X-ray wavelength, Dp the angular line width of half maximum intensity and θ is the Bragg angle in degrees. The particle size of $Mn_xZn_{(1-x)}$ Fe_2O_4, where x= 0.4, 0.5, 0.6, 0.7 and 0.8 with Mn concentration is given in Table 2. The crystallite sizes are found to increase with increasing Mn content in the range 20.4– 41.1 nm for different compositions. It is observed that minimum crystallite size of 20.4 nm is observed for the ferrite sample with Mn concentration of x=0.4 which may be due to the lower concentration of Mn ions and as the concentration of manganese increases which have higher ionic radii (0.91Å), compared to zinc ions (0.82Å) the lattice constant increases and also crystallite size increases.

Table 2: Variation of particle size in nm

Concentration of Mn	Particle size in nm
0.4	20.4
0.5	21.9
0.6	34.1
0.7	38.6
0.8	41.1

From the figures 3(a), (b) and (c), the microstructure of Mn-Zn ferrites reveals that the nanoparticles are porous and are agglomerated due to the presence of magnetic interactions.

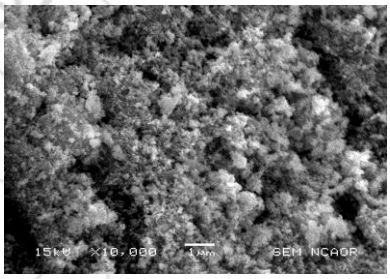

(a)

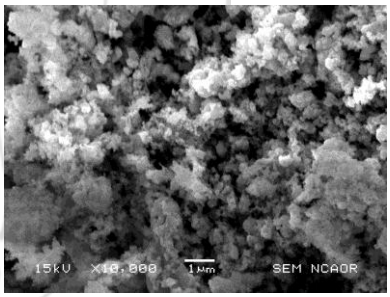

(b)

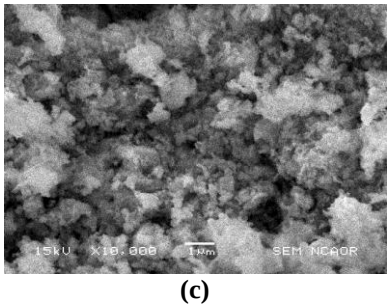

(c)

Figure 3: SEM micrograph of (a) $Mn_{0.4}Zn_{0.6}Fe_2O_4$, (b) $Mn_{0.6}Zn_{0.4}Fe_2O_4$ & (c) $Mn_{0.8}Zn_{0.2}Fe_2O_4$.

The variation of the saturation magnetization with Mn contents for the Mn-Zn ferrite samples of various compositions is given in Table 3. It can be observed that the value for saturation magnetization (Ms) increases with increasing Mn ion content. Till x = 0.6 and thereafter for x =

0.7 and 0.8 it is found to decrease. According to Costa [9], this behavior can be attributed to the „„spin canting"" effect that occurs when B-B interactions are comparable to A-B interactions. Bercoff et al. [10] explains this phenomenon in mixed Ni–Zn ferrites, in which the Zn^{2+} ions concentrate preferentially in the A sites and the Ni^{2+} ions in the B sites in the cubic spinel lattice. When the concentration of Fe^{3+} ions in the A sub-lattice is diluted by low concentrations of diamagnetic substitutions (such as Zn^{2+}), the net magnetization increases. However, magnetization decreases at higher levels of doping. The reason for this is that low Zn concentrations reduce the number of spins occupying the A sublattices, causing the net magnetization to increase. As the Zn content increases, the exchange interactions are weakened and the B spins are no longer held rigidly parallel to the few remaining A spins. The decrease in the B-sublattice moment, interpreted as a spin departure from colinearity, causes the effect known as canting. Sattar et al.[11] also described this effect in samples of Cu–Zn ferrites at concentrations of Zn^{2+} exceeding 0.4% in mol. The Ms is minimum for $Mn_{0.4}Zn_{0.6}Fe_2O_4$ i.e. 21.74 emu/g and maximum for $Mn_{0.6}Zn_{0.4}Fe_2O_4$ i.e. 45.17 emu/g. respectively. The hysteresis loss is found to be low for all the samples.

Table 3: Variation of saturation magnetization

Composition	*Saturation Magnetization (emu/g)*
$Mn_{0.4}Zn_{0.6}Fe_2O_4$	21.74
$Mn_{0.5}Zn_{0.5}Fe_2O_4$	36.52
$Mn_{0.6}Zn_{0.4}Fe_2O_4$	45.17
$Mn_{0.7}Zn_{0.3}Fe_2O_4$	38,91
$Mn_{0.8}Zn_{0.2}Fe_2O_4$	33.11

Table 4: Variation of curie temperature

Composition	*Curie temperature in ^0C*
$Mn_{0.4}Zn_{0.6}Fe_2O_4$	232
$Mn_{0.5}Zn_{0.5}Fe_2O_4$	257
$Mn_{0.6}Zn_{0.4}Fe_2O_4$	289
$Mn_{0.7}Zn_{0.3}Fe_2O_4$	341
$Mn_{0.8}Zn_{0.2}Fe_2O_4$	384

The Curie temperature was found to increase with increase in manganese content in the samples $Mn_{0.4}Zn_{0.6}Fe_2O_4$ to $Mn_{0.8}Zn_{0.2}Fe_2O_4$ from 232 ^{0}C to 384 ^{0}C as given in Table 4, in these ferrites [12]. This is attributed to the substitution of non-magnetic Zn^{2+} ions by the magnetic Mn^{2+} ions in the samples. The value of Tc is found to be higher in the case of the nanoparticles than that in bulk ferrites. This is due to the deviation of cation distribution in a nano-sized particle as in comparison with its bulk counterparts [13]. In general, magnetic properties are controlled by exchange interaction of the metallic ions on the two interactive sub-lattices A and B. It is also possible that Tc may decrease due to some unknown surface effect. For small particles a significant fraction of atoms are on the surface, and therefore their magnetic interactions is expected to be different. It is observed to give rise to a different average Curie temperature [14].

4. Conclusion

The samples $Mn_xZn_{1-x}Fe_2O_4$ with x=0.4, 0.5, 0.6, 0.7 and 0.8 prepared by using Succinate hydrazinate ligand with metal ions to produce a precursor, which undergoes auto combustion- self decomposition, were found to have spinel structure. This was confirmed using XRD and IR spectroscopy. The particle sizes were estimated using Scherer formula and were found to be in nano range, confirmed by SEM. Nano-materials produced by this method show high values of saturation magnetization. Tc increases with Mn content and was found to be higher than for the bulk material.

References

[1] M. Atif, M. Nadeem, R. Grossinger, R. S. Turtelli, "Studies on the magnetic, magnetostrictive and electrical properties of sol–gel synthe-sized Zn doped nickel ferrite", Journal of Alloys and Compounds 509 (2011) 5720–5724.
[2] C. C. Hwang, J. S. Tsai, T. H. Huang, "Combustion synthesis of Ni–Zn ferrite by using glycine and metal nitrates-investigations of precursor homogeneity, product reproducibility, and reaction mechanism", Materials Chemistry and Physics 93(2005) 330–336.
[3] T. Slatineanu, A. R. Iordan, M. N. Palamaru, O. F. Caltun, V. Gafton, L. Leontie, "Synthesis and characterization of nanocrystalline Zn ferrites substituted with Ni, Materials Research Bulletin 46 (2011) 1455–1460.
[4] K. H. J. Buschow, Concise Encyclopedia of Magnetic and Superconducting Materials, Elsevier Science, 2005
[5] M. R. Syue, F. J. Wei, C. S. Chou, C. M. Fu, Magnetic, dielectric, and complex impedance properties of nanocrystalline Mn–Zn ferrites prepared by novel combustion method, Thin Solid Films 519 (2011) 8303–8306.
[6] R. Gimenes, M. R. Baldissera, M. R. A. da Silva , C. A. da Silveira , D. A.W. Soares, L. A. Perazolli, M. R. da Silva, M. A. Zaghete Ceramics International 38 (2012) 741–746
[7] R. D. Waldron. *Phys. Rev.*, **1955**, 99, 1727
[8] Thanit Tangcharoen,, Anucha Ruangphanit, Wisanu Pecharapaa, Ceramics International 39 (2013) S239–S243
[9] A.C.F.M. Costa. Synthesis for Combustion Reaction, Sinterizaction and Ferrites Characterization Ni–Zn Thesis (Doctorate in Sciences and Engineering of Materials) Department of Engineering of Materials, Federal University of São Carlos, São Carlos, 2002.
[10] P. G. Bercoff, et al., J. Magn. Magn. Mater. 213 (2000) 56.
[11] A. A. Sattar, et al., Phys. State Solid 171 (1999) 563.
[12] R. Iyer, R. Desai, R. V. Upadhyay, Bull. Mater. Sci., 32 2, (2009) pp. 141–147.
[13] C. Rath, S. Anand, R. P. Das , J. App. Phys. 91(2002) 2211.
[14] J. P. Chen, C. M. Sorenson, K. J. Klabunde, G. G. Hadjipanayis, E. Delvin, A. Kostidas, Phys. Rev. B54 (1996) 9288.